

Design of a Microgrid-based DC Smart Home

Gareth Jones

Hydramatics Control Equipment CC
South Africa

Email: gjones@hydramatics.co.za

Ewald Erasmus

University Of Pretoria
South Africa

Email: Ewald.Erasmus@outlook.com

Abstract— In order to reduce the overall load of households on the electrical utility network, a DC based microgrid home is proposed. This paper explores the concept, design as well as construction of two DC-DC converters which were used to realise a scalable model of this system. The selected distribution voltage was 48 V, selected for its ability to supply higher power appliances while still remaining within the range of extra low voltage. To interface with these appliances, a versatile socket was proposed. The design topology chosen for the socket was a full-bridge DC-DC converter with adjustable PWM control. The converter topology was chosen due to its ability to provide isolation between the supply and the load while still being able to supply higher power applications. Another converter was designed for the charging of the battery bank. This converter was realised using a synchronous buck topology, chosen for its high efficiency as well as scalability. A hybrid MPPT/Multistage charging algorithm was designed for the efficient transfer of power between the PV panels and batteries. The implementation of the converters proved to be successful with both converters displaying efficiencies well above 90%. The charging algorithm was able to not only charge the battery in a safe and effective way but was also able to maximise the output of the PV panel during the bulking phases of charging.

Index Terms- Smart home; DC microgrid; variable DC-DC converter; MPPT charger; Converter design; DC distribution

I. PROBLEM IDENTIFICATION AND BACKGROUND

The quest to use more sustainable and renewable energy sources is a popular topic and goal of many government organisations. The motivation behind this quest is to preserve the environment and to use its resources more efficiently and conservatively. The creation of microgrids with localised generation and storage has become popular practice in many nations where fossil fuels are being phased-out and replaced with renewables [1].

The DC microgrid topology aims to support this pursuit by providing a relatively simple means of localised power generation that can directly feed the local power users more efficiently. Many household appliances are in fact DC appliances adapted to suit the existing AC distribution of the national grid [2]. While this is the current norm, alternative solutions need to be investigated to ensure that the most efficient and sustainable technologies are being implemented.

The most commonly implemented microgrid topology to date is the AC variant. In this topology, a source (often renewable, as shown in Fig. 1) is connected to a storage device via a charge controller. The stored power is then amplified and inverted into conventional mains power (AC). When a load is

connected, it typically converts the AC power back into DC power before being used. This flow of power is shown in Fig. 1.

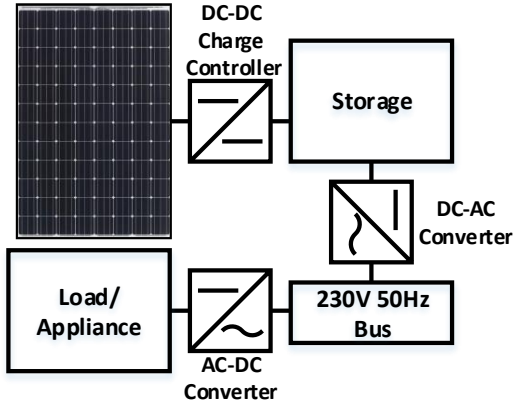


Figure 1: AC Microgrid Topology

A DC microgrid, on the other hand, takes advantage of the DC nature of household appliances, avoiding the excessive DC-AC and AC-DC conversions that are necessary in an AC microgrid. By supplying the loads with DC power, as shown in Fig. 2, the overall efficiency of the system should increase as well as alleviating the need for inverters and rectifiers within the network.

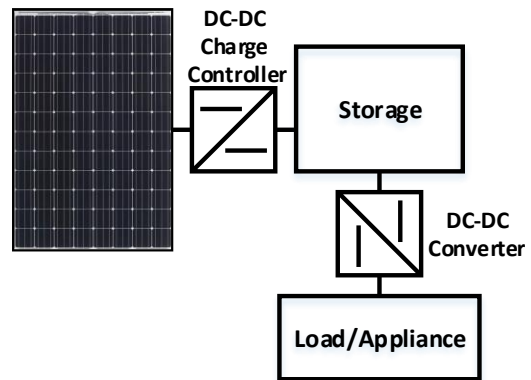


Figure 2: DC Microgrid Topology

With the growing interest in renewable energy, engineers are looking for optimal solutions to improve the reliability and capability of future power grids. Some of the advantages and challenges of DC distribution systems is uncovered in [3]. In an effort to move towards a more reliable and economical power grid, it is important to explore the potential of completely DC-based grids. However, there is an inevitable transition period where AC and DC grids need to be interfaced, and standards

still need to be established for DC distribution networks. These standards are currently being investigated and pursued by the EMerge Alliance association [2], but these are not (yet) common practice as DC distribution microgrids are being installed and operated privately, without much regulation, unless they are exporting power to a utility's distribution network.

The benefits of a microgrid are numerous as discussed in [4], as well as promoting greater awareness of energy consumption as the system capacity needs to be designed based on load requirements and it needs to be continuously monitored once in operation. This promotes smart metering and control of devices, which can lead to more conservative energy consumption worldwide. The economical, commercial and environmental benefits of DC microgrids are clear. However, it is important to explore the challenges of DC distribution as the opportunity for implementing these systems is growing.

II. METHODS

The project presented here entails the design and implementation of a DC microgrid with a focus on a variable DC-DC power outlet or “socket” converter that is able to handle a varying range of DC voltages. The converter has a simple user interface in order to select the desired output voltage of the socket. Another DC-DC converter is required to perform the task of charging a battery bank from a solar PV array. This charger converter implements an MPPT charging algorithm to maximise the panel output power and charge the batteries effectively. The bus voltage for the system was selected as 48 V with the expectation of reducing system losses and allowing for more efficient operation for higher power applications [5].

The project is a system of multiple components, in which each aspect of each component needs to be designed and reviewed in order to achieve the optimal solution. There is a lot of literature pertaining to each aspect of the project, as well as the system as a whole. The focus of this review was converter topologies and components. It was necessary to determine the optimum methods of design and construction of these devices.

I. Converter Design

Two DC-DC converters were required to realise the system. The converters were designed from first principles, including the magnetic design of the high-frequency inductors and the isolation transformer. Semiconductor devices were also sized

according to calculated ratings, including a safety factor. An initial design decision was made to implement a switching frequency of 50 kHz for both converters. It was desirable and economical to specify as many similar components as possible for both converter designs. The mathematical calculations were performed with software so that they could be easily updated once specific components were procured. The theoretical calculations were then simulated using PSIM to gain insight into the actual operation of the converters.

Alternative topologies were compared and the full-bridge topology was selected for the socket converter, due to high power capability (for future work) as well as for the isolation it provides between the source and the load. The circuit schematic is shown in Fig. 3. The detailed procedure of calculations is excluded from this summary, but the calculated design parameters for components are shown in Table 1. The full-bridge topology is suitable for applications requiring power greater than 10 kW, however, in this proof of concept design, the power capacity was set to 250 W, which can be increased in future work without changing the type of topology.

Table 1: Socket converter component design

Parameter/ Component	Result	Rating used (with safety factor)
L_{out}	154 μ H	200 μ H (built)
C_{out}	8.68 μ F	47 μ F
V_{co}	60-72 V	100 V
C_{in}	492 μ F	470 μ F
V_{ci}	75-90 V	100 V
$I_{sw,rms}$	19.7 A	29.55 - 39.4 A
V_{sw}	56.98 V	85.46 – 113.95 V
$I_{D,rms}$	11.46 A	17.18 - 22.91 A
V_D	137.9 V	206.86 – 275.81 V

An important specification was that of the switching semiconductor devices. After reviewing literature, it was determined that a MOSFET would be the ideal type of switch for the application. Selecting the right MOSFET was based on the voltage and current requirements recorded in Table 1, but ultimately it was desirable to find the MOSFET with the lowest drain-to-source resistance, $R_{DS(on)}$, value, which assists in reducing the heat loss of the device, thus improving its efficiency. The specification of the rectifying diode was similar in that finding the lowest forward voltage, V_F , was required.

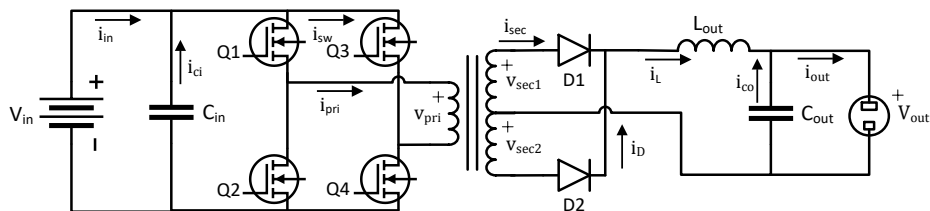


Figure 3: Socket converter full-bridge topology

The most suitable MOSFET and diode sourced for the project were:

- MOSFET: IRFB4321PbF ($R_{DS(on)} = 12 - 15 \text{ m}\Omega$) [6]
- Diode: STPS80170C ($V_{F,max} = 0.74 \text{ V}$) [7]

A magnetic design procedure was also conducted for the inductor and transformer specification. The complete design procedure is omitted from this summary, but the inductor of $200 \mu\text{H}$ and a transformer large enough to handle the power requirements were constructed.

A simpler synchronous buck topology was selected for the charger converter as it was deemed suitable to handle rated power of the available solar PV panels. A synchronous buck was chosen over a non-synchronous type, due to the higher efficiency expectations. Figure 4 below shows the topology of the converter. Calculations, not shown here, were completed to obtain component values, based on a maximum desired output power of 400 W.

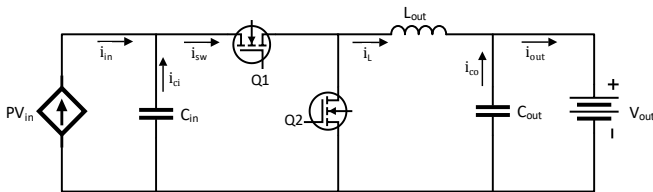


Figure 4: Charger converter synchronous buck topology

A summary of some important component parameters is shown in Table 2 below.

Table 2: Charger converter component design

Parameter/Component	Result	Rating used (with safety factor)
L_{out}	$784 \mu\text{H}$	$770 \mu\text{H}$ (built)
C_{out}	$11.16 \mu\text{F}$	$22 \mu\text{F}$
V_{co}	$72.5-87 \text{ V}$	100 V
C_{in}	$72.57 \mu\text{F}$	$100 \mu\text{F}$
V_{ci}	$105-126 \text{ V}$	160 V
$I_{sw,rms}$	8.19 A	$12.28-16.38 \text{ A}$
V_{sw}	84.13 V	$126.19-168.25 \text{ V}$

Based on the calculations summarised above, it was determined that the same MOSFET specified for the socket converter could be used for the charger as well, although it provided a safety factor of only 1.78 rather than greater than 2.0. The inductor design for the charger converter was also completed, but the constructed device fell slightly short of the calculated value, despite adjusting the airgap, due to mechanical tolerances. Both converters were simulated in PSIM to check the calculations and gain insight into the dynamic operation of the converter, before being assembled on PCB board. Component placement and trace lengths were important considerations and every effort was made to optimise the distance and shape of the trace between critical components, which reduced unnecessary heat loss. EMI concerns were also carefully considered with reference to [8], although most signals were below 50 kHz, frequency doubling at the output of

the socket converter resulted in 100 kHz also being present on the board.

In order to achieve well-functioning system, it was important to focus on each component that contributed to the system. Some important design choices and component specifications are discussed below.

1) MOSFET driver circuitry

The MOSFET was selected for its low drain-source resistance and quick rise and fall times. A suitable driver to complement this MOSFET was required. The HCPL3120 was chosen as the right driver for the application. It provided isolation between the microcontroller and MOSFET gate, while keeping delay time to a minimum. The delay time of the driver was not as short as the MOSFET but this was consistent as each switch had its own driver. Component operating tolerances always have an effect, but using good quality components ensured that these were kept to a minimum. The driver circuit implemented in both converters is shown in Fig. 5. It is important to note that separate power supplies were used for each of the high-side switches and another for the low-side switches, where applicable. This is one way to avoid short-circuits, but not necessarily the most economical. Other methods were considered with reference to [9], but the simplest solution was selected for this prototype.

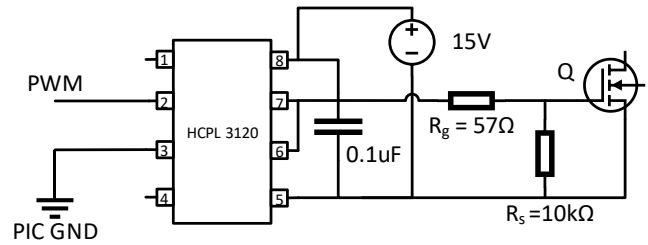


Figure 5: MOSFET driver circuit

2) Microcontroller and sensors

The control circuitry and components were just as important as the power circuitry. The converter operation is dependent on PWM control and feedback via voltage and current sensors. A dsPIC33F microcontroller was selected to control the converters of this project. It was designed for PWM control and has an on-board ADC for sensors. This allowed for simple coding to achieve rudimentary PID control of the PWM signal, by manipulating the dead-time between the two (pairs of) switches. A single PCB was designed to accommodate the dsPIC, voltage sensors as well as auxiliary supplies for the HCPL3120 drivers. This single board kept the overall system compact and made testing and troubleshooting easier. The voltage sensors were also kept far away from PWM switching noise and high power traces, interfacing to the power circuitry via two jumper leads. The current sensors were packaged on a breakout board and thus needed to connect in line with power traces, but they were well isolated. The sensors were calibrated in-circuit to ensure that accurate ADC readings could be obtained.

III. RESULTS

The converters were successfully designed and built according to the theoretical calculations. The testing of both converters was conducted to check that all specifications were met. The power rating of the socket converter was achieved, as shown in the two oscilloscope images, Fig.6 and Fig.7, which show the input and output voltage and current waveforms, respectively. The recorded efficiency at this operating power was 82.4 %, but other tests at lower power revealed efficiencies above 90 %.

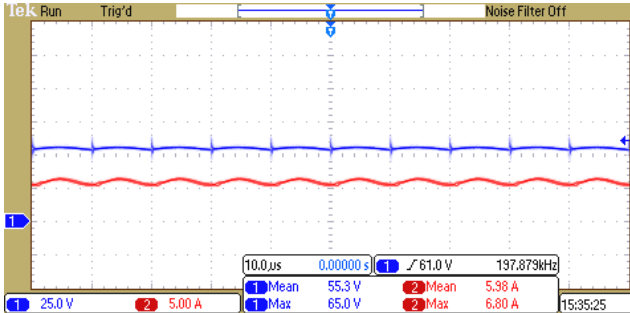


Figure 6: Socket converter input voltage and current for Pin = 295 W

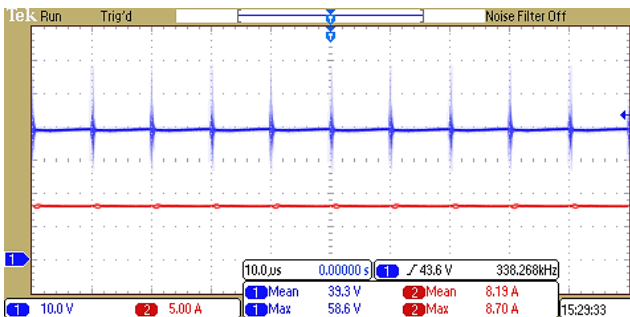


Figure 7: Socket converter output voltage and current for Pout = 243 W

The output power rating of the charger converter was tested up to 345 W, often showing efficiencies greater than 90 %, although the waveforms of lower tests are shown in Fig. 8 and Fig. 9 below. Note that only the output voltage was displayed during the test with a voltage probe that had a DC offset. Thus, all voltage measurements were verified with a multimeter that has a 100 kHz bandwidth to calculate a more accurate power value. The efficiency of the converter in this test was 97 %. The converter could withstand the higher power tests safely, without overheating or failing. The voltage spikes seen in Fig. 7 occurred as expected, based on the switching frequency of 50 kHz. This frequency is effectively doubled at the output due to the rectification stage using a centre-tapped transformer. The voltage spikes are shown to be about 50 % of the mean value, which is certainly more than desired. Snubber circuits were investigated to combat this [10], which reduced overshoots in some cases, but seemed to increase them at other settings. The snubber circuits were ultimately removed, but this could be investigated further and improved upon in future work.

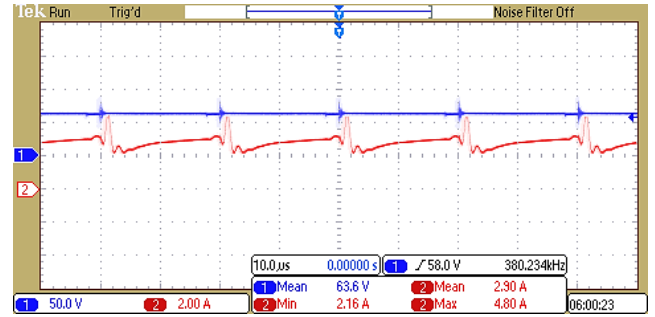


Figure 8: Charger converter output voltage and input current for Pin = 180 W

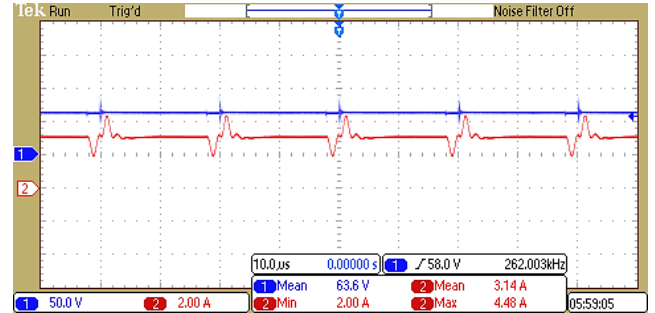


Figure 9: Charger converter output voltage and output current for Pout = 175 W

The control algorithm used for the MPPT charge controller was developed in a robust and simple manner, which prioritised the health of the battery. The compromise with this approach was that the maximum power would not be drawn from the PV panel at all times. Therefore, the control algorithm was rather a hybrid between MPPT and multistage charging. A basic overview of the algorithm is shown in Fig. 10.

The results using this algorithm were satisfactory, with the various charging phases being demonstrated clearly. The charger not only effectively charged the battery, but also stopped the battery from overcharging. The algorithm also created a safeguard for the battery preventing the battery from entering an excessive gassing phase. A challenging aspect was determining the state of charge (SOC) of the battery, however, it was found that measuring the terminal voltage provided a good estimation of the initial SOC as long as the battery had been at rest for some time between tests (± 30 minutes). Measurements during operation were also negatively affected by voltage spikes in the converter output. This required some adjustments to the ADC sampling code to ensure that these spikes did not cause an incorrect change in the charging phase.

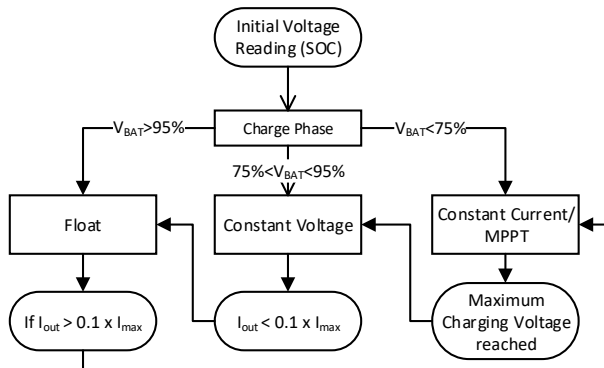


Figure 10: Charge Algorithm Flow Diagram

The efficiency of both converters exceeded expectations, as both were capable of operating at efficiencies above 85 %, although the power consumption of the auxiliary supplies was not included in efficiency calculations.

PV panel and battery sizing for the system was also conducted successfully, but only available equipment was used for testing purposes.

Photos of the two completed converters (prior to boxing) are shown below. The PIC and sensor boards were sized correctly so that they could be stacked neatly above the power circuitry.

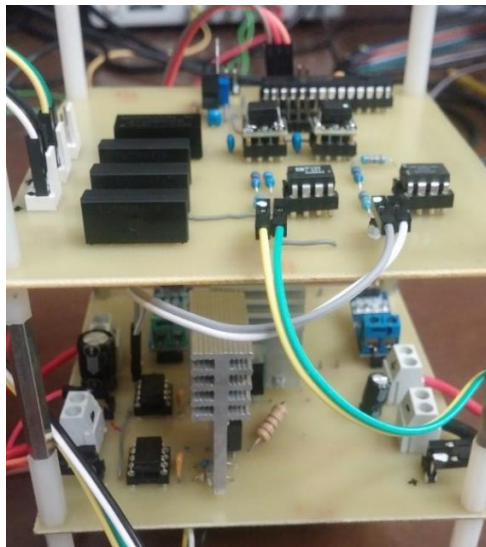


Figure 11: Completed charger converter



Figure 12: Completed socket converter

IV. DISCUSSION AND CONCLUSION

This project presented a first attempt at designing, constructing and testing DC-DC converters. A few iterations were required to achieve acceptable results, but eventually, successful results were achieved. The testing protocols allowed for individual components or sub-circuits to be tested before completing system tests. This was a safe and systematic approach to realise the final system.

The calculated parameters and component specifications performed well in practice. It was clear that certain aspects required an iterative design process as components were integrated into systems. Selecting the right component for an application was found to be a critical stage of the process to reduce system inefficiencies and ensure safe operation. For example, the very low drain-to-source resistance of the MOSFET reduced heat loss and therefore improved the efficiency of the system.

The testing of the converters revealed surprising results regarding efficiency. The measurement probes in the laboratory were not perfect and discrepancies between measurements were expected. However, the results showed very promising operating efficiencies of both converters.

A good PCB layout was another important contributing factor to system efficiency. Component placement was carefully considered in order to reduce trace losses and control signal latency, as well as EMI in some cases. The control and sensor board layout was designed to improve noise rejection.

The PWM control of the socket converter functioned well, but it could certainly be improved with a better user interface. The control algorithm can also be tuned further to achieve better set point tracking and reduce steady state error, especially with a varying load. The control was a challenging aspect of the design; although perfecting the hardware was an extensive challenge, the device could not operate if it could not be controlled. The coding of the control algorithms was not always successful and the debugging process was time-consuming.

The chosen bus voltage of the system proved to be advantageous in achieving higher power output from the converters. It was difficult to test such low resistance loads to achieve desired power ratings at lower voltages. The 48 V bus was suitable in terms of safety and efficiency in laboratory testing conditions.

Although the project involved a complete microgrid system, the design and development of DC-DC converters was a central focus. The design required great attention to detail for the many intricate components. All converter specifications were calculated and appropriate components were specified, allowing for necessary safety factors. The converter circuitry was designed and implemented on PCB. Control of the circuitry, including MOSFET switching, and voltage and current sensing, was achieved using a dsPIC coded in C programming language. Converter hardware performed well to meet the specifications and in fact exceeded expectations in terms of efficiency. A hybrid form of a MPPT/charging control algorithm was implemented successfully although the method for detecting the battery SOC needs to be improved. The socket converter was able to maintain a set point output voltage with reasonable accuracy, using a basic form of PID control to adjust the dead time of PWM signals. As a whole, the system proved to be viable. With some further integration between the components and better energy management features, this would certainly be effective for setting up a small DC microgrid in which devices with varying voltage requirements could be operated successfully. This can certainly be developed further with more advanced converters, allowing focus to shift more towards designing, operating and managing the microgrid as a whole, rather than only controlling the converters. In line with the current trend of IoT devices and systems, this DC microgrid could provide a feasible power solution in both rural and city households. With intelligent power outlets communicating with intelligent battery chargers, the system can be managed very safely and efficiently. This communication naturally extends to neighbourhoods for larger microgrids as well.

V. ACKNOWLEDGMENTS

The authors would like to thank Dr R. Naidoo (University of Pretoria) for his guidance in the research, as well as SANEDI for their continual funding.

REFERENCES

- [1] G. Venkataraman and C. Marnay, "A Larger Role for Microgrids," *IEEE Power Energy Mag.*, vol. 6, no. june, pp. 54–65, 2008.
- [2] K. Garbesi, V. Vossos, H. Shen, J. Taylor, and G. Burch, "Catalog of DC Appliances and Power Systems," Lawrence Berkeley National Laboratory, Berkeley, 2011.
- [3] L. Mackay, T. G. Hailu, G. C. Mouli, L. Ramirez-Elizondo, J. A. Ferreira, and P. Bauer, "From DC nano- and microgrids towards the universal DC distribution system - A plea to think further into the future," *IEEE Power Energy Soc. Gen. Meet.*, vol. 2015–Septe, 2015.
- [4] A. Khodaei, M. Shahidehpour, and R. W. Galvin, "Microgrid-Based Co-Optimization of Generation and Transmission Planning in Power Systems," *IEEE Trans. POWER Syst.*, vol. 28, no. 2, 2013.
- [5] W. Li, X. Mou, Y. Zhou, and C. Marnay, "On voltage standards for DC home microgrids energized by distributed sources," in *Conference Proceedings - 2012 IEEE 7th International Power Electronics and Motion Control Conference - ECCE Asia, IPEMC 2012*, 2012.
- [6] International Rectifier, "IRFB4321PbF," www.irf.com, 2008.
- [7] [Online]. Available: <http://docs-europe.electrocomponents.com/webdocs/0b3c/0900766b80b3c196.pdf>. [Accessed: 28-Jul-2016].
- [8] STMicroelectronics, "STPS80170C - HIGH VOLTAGE POWER SCHOTTKY RECTIFIER." p. 6, 2005.
- [9] Texas Instruments Inc., "PCB Design Guidelines For Reduced EMI." Texas Instruments Incorporated, p. 23, 1999.
- [10] J. Formenti and R. Martinez, "Design Trade-offs for Switch-Mode Battery Chargers," 2004..
- [11] R. Severns, "DESIGN OF SNUBBERS FOR POWER CIRCUITS." p. 29.